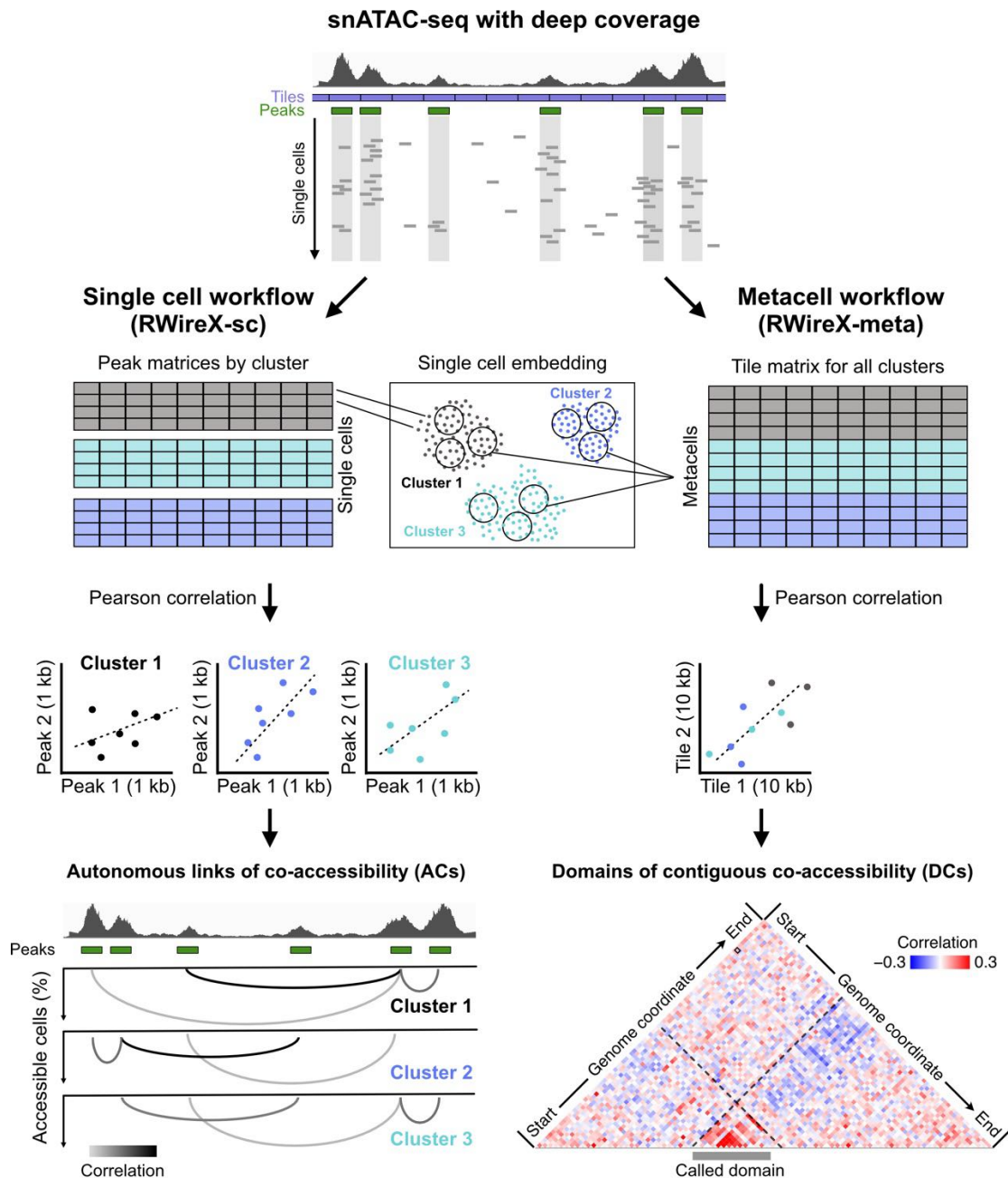
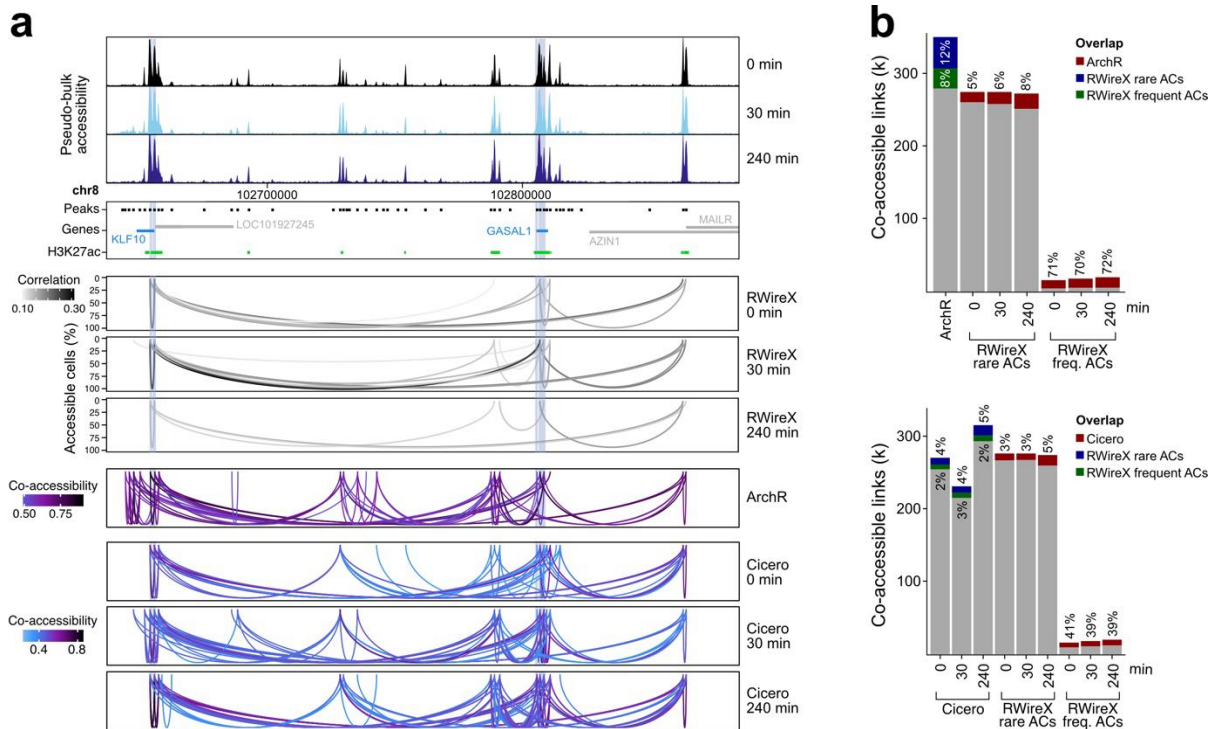

Two distinct chromatin modules regulate proinflammatory gene expression

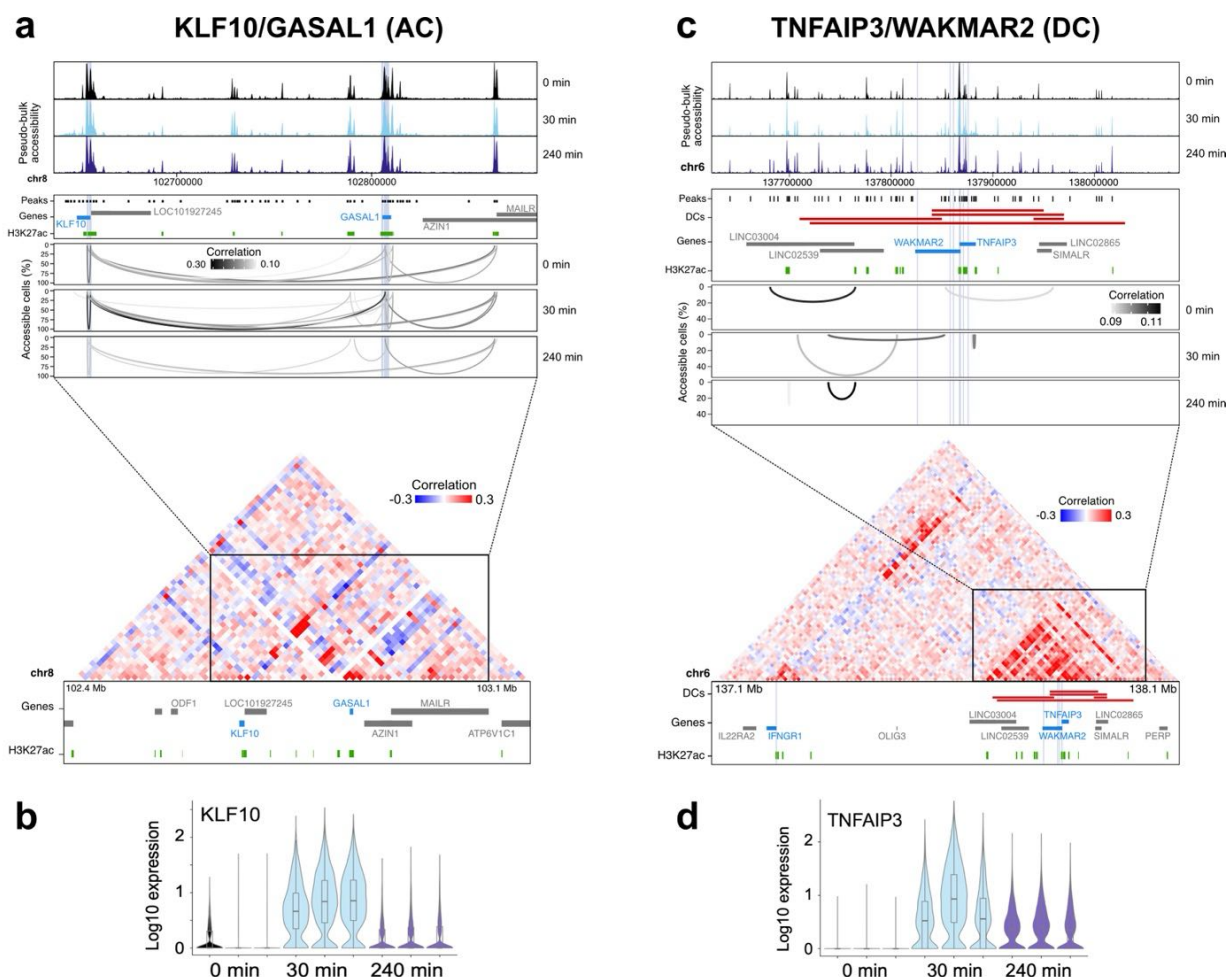
In the format provided by the
authors and unedited



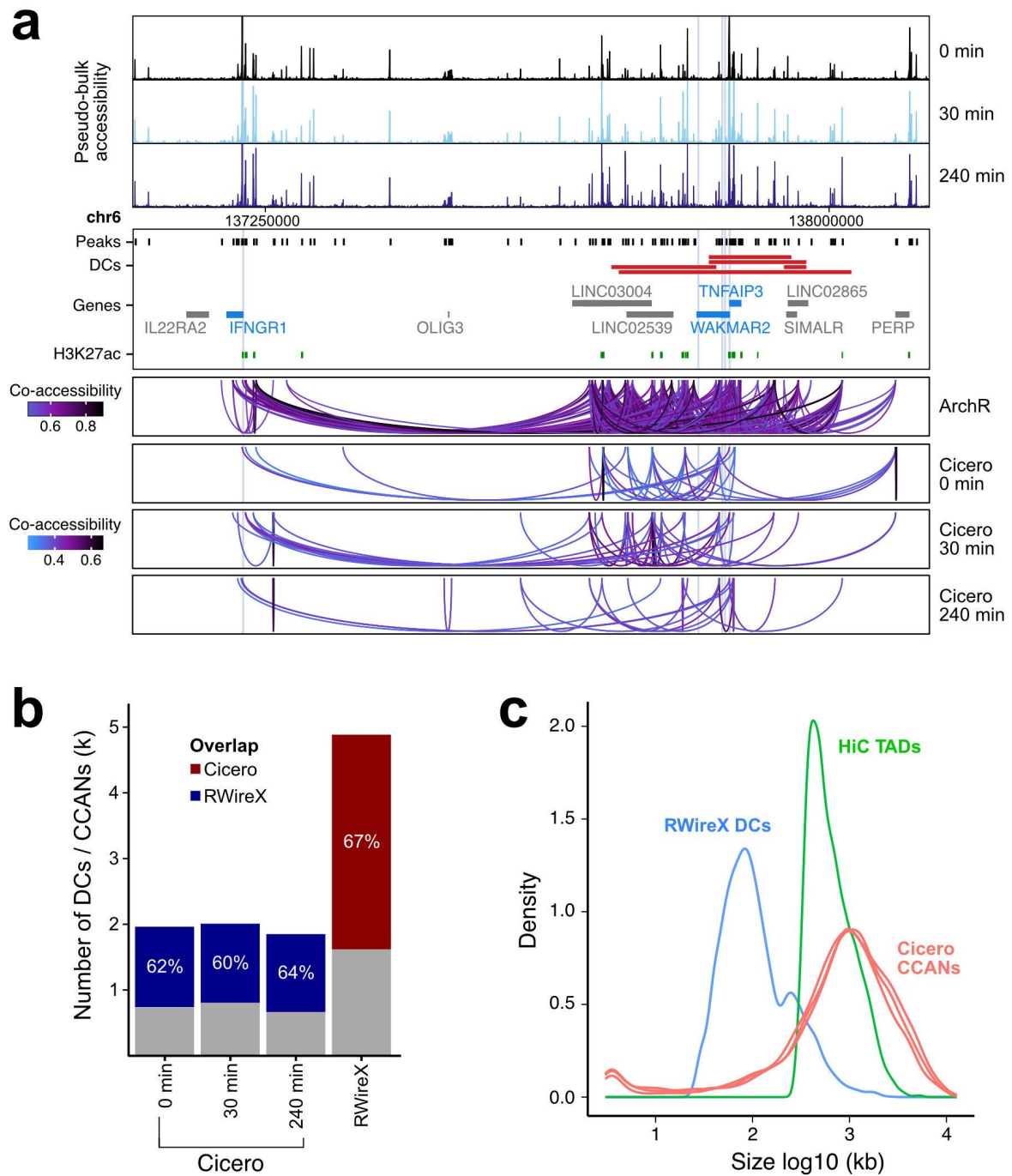
Supplementary Fig. 1. Detailed RWireX analysis workflow. RWireX computes co-accessibility from snATAC-seq data using two distinct workflows to resolve different layers of chromatin accessibility variation. It is implemented as an extension of ArchR and is available at <https://github.com/RippeLab/RWireX>. Left: Single-cell co-accessibility workflow (RWireX-sc). This workflow requires a homogeneous cell population as input (e.g., individual time points or cell-type clusters) to resolve stochastic changes in co-accessibility, since the signal would otherwise be confounded by cell-state/type differences in a heterogeneous population. RWireX-sc yields autonomous links of co-accessibility (ACs) from Pearson correlation coefficients, reflecting transient changes in co-accessibility between 1-2 kb regions around ATAC peaks across single cells. The grey levels of the arcs indicate the magnitude of the Pearson correlation coefficient between the two peaks. In contrast, the height of the arcs indicates the link activity, defined as the average percentage of cells in which at least one of the linked peaks is accessible. Right: Metacell co-accessibility workflow (RWireX-meta). This workflow requires heterogeneous cell populations (e.g., different cell states/types) as input to map broader domains that display coordinated accessibility changes within the cell population. These domains of contiguous co-accessibility (DCs) are computed from changes in accessibility within 10 kb genomic tiles across metacells, which are aggregated from cells with similar chromatin accessibility profiles. DCs are determined from the metacell co-accessibility matrices using hierarchical domain calling for both small domains (minimal size 20 kb, window 200 kb) and large domains (minimum size 200 kb, window 2 Mb). The overall co-accessibility of domains is given by the average Pearson correlation coefficient within the domain.



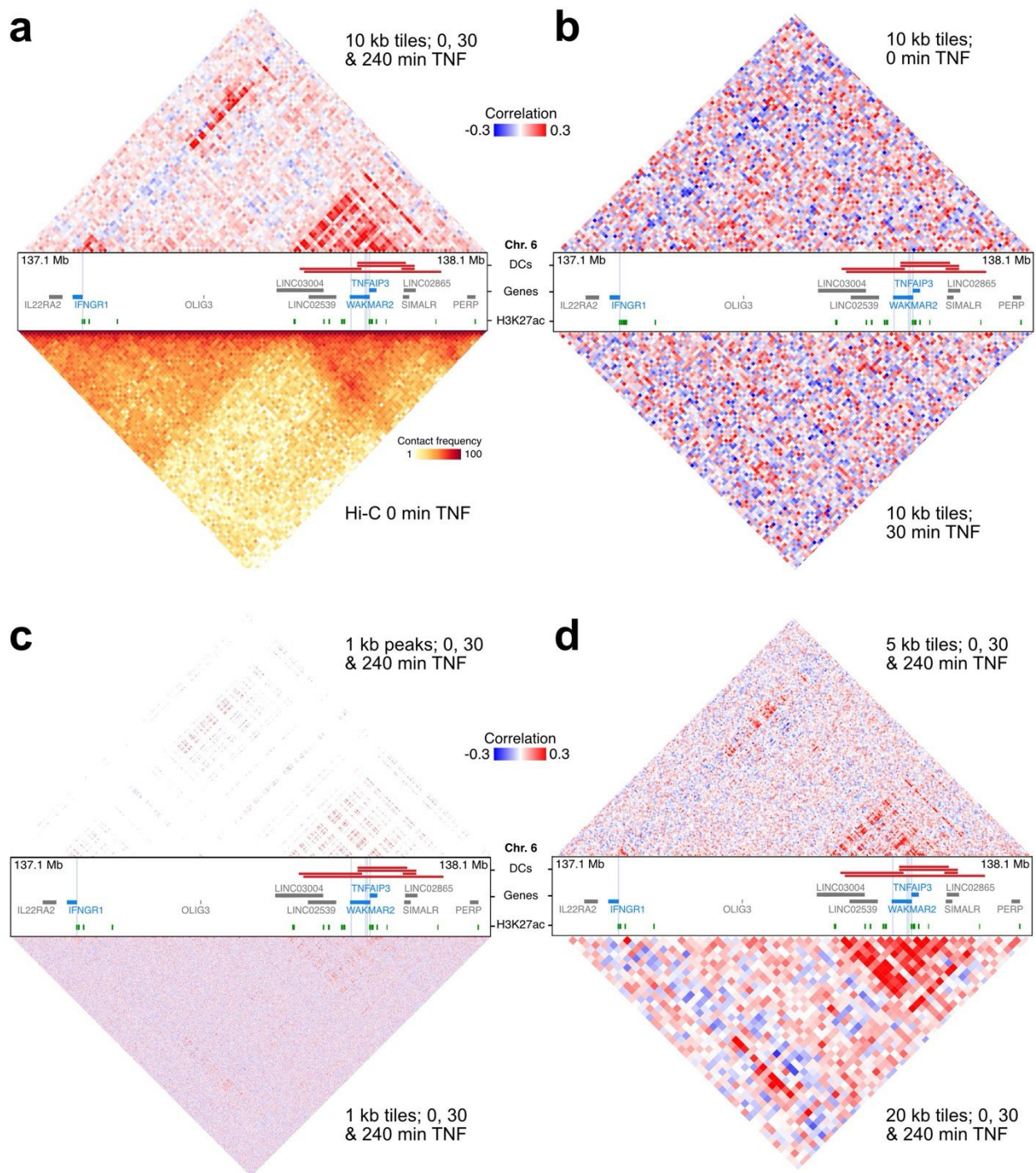
Supplementary Fig. 2. Comparison of co-accessibility analyses using ArchR, Cicero, and RWireX at the *KLF10/GASAL1* TRG cluster. At this locus the simultaneous presence of ATAC and H3K27ac is detected only at the promoters of the TRGs *KLF10* and *GASAL1*, along with a bona fide enhancer downstream of *GASAL1* that features a cluster of three adjacent peaks (chr8: 102,862,153-102,863,057; chr8: 102,863,125-102,863,598; chr8: 102,863,652-102,865,276) and one located between the two genes (chr8:102,787,594-102,791,222). Data from replicate 1 of snATAC-seq was utilized. **(a)** ArchR and Cicero co-accessibility at the *KLF10/GASAL1* TRG cluster. Top: pseudo-bulk chromatin accessibility. Top: pseudo-bulk ATAC peaks extended to 1 kb (black), H3K27ac peaks at 30 minutes TNF (green), TRGs (blue), 1 kb regions surrounding their TSSs (light blue), and other genes (grey). Middle: ACs at TRG promoters identified from RWireX-sc co-accessibility. Co-accessible links are visualized as arcs. The grey level indicates the magnitude of the correlation between the two peaks, and the height of the arcs indicates the percentage of cells in which one or both sites were accessible. Bottom: Co-accessibility links across all conditions from ArchR and per condition from Cicero. ArchR identified co-accessibility links between the two H3K27ac-marked enhancers, the *KLF10* and *GASAL1* promoters, as well as multiple other peaks in the genomic region that were absent in the RWireX-sc analysis. Similarly, Cicero detected co-accessibility links between the two H3K27ac-marked enhancers, the *KLF10* and *GASAL1* promoters, along with numerous other peaks. This comparison indicates that the analysis of metacells done in Cicero and ArchR is unsuitable for the purpose of detecting stochastically occurring co-accessibility changes, as aggregating single cells results in a loss of this information, particularly for less frequent events **(b)** Number of co-accessibility links from ArchR (top) and Cicero (bottom), and rare/frequent ACs from RWireX-sc. Colors indicate the overlap between links detected by ArchR and RWireX-sc. This genome-wide comparison revealed that ArchR co-accessibility links overlapped with only 5-12% of rare ACs from RWireX-sc but recovered 70-72% of frequent ACs. Similarly, Cicero showed 3-5% overlap with rare ACs and 39-41% recovery of frequent ACs from RWireX-sc. While ArchR and Cicero identify frequent ACs with greater sensitivity, they exhibit lower specificity (5.2-fold and 3.8-fold more total links called, respectively) and fail to resolve rare ACs.



Supplementary Fig. 3. Comparison of RWireX-sc and RWireX-meta co-accessibility analyses at the *KLF10/GASAL1* and the *TNFAIP3/WAKMAR2* TRG clusters. (a) RWireX co-accessibility of the *KLF10/GASAL1* TRGs (blue) together with pseudo-bulk ATAC chromatin accessibility and H3K27ac peaks at 30 min (green). Top: RWireX-sc analysis to map ACs at TRG promoters. Multiple promoter-linked ACs are present for *KLF10* and *GASAL1*. Bottom: RWireX-meta co-accessibility showing that no DC is detected for these TRGs. (b) Gene expression of *KLF10* TRG. (c) RWireX co-accessibility of the *TNFAIP3*, *IFNGR1*, and *WAKMAR2* TRGs (blue) together with pseudo-bulk ATAC chromatin accessibility and H3K27ac peaks at 30 min (green). Top: RWireX-sc analysis to map ACs at TRG promoters. No promoter-linked ACs were detected. Bottom: RWireX-meta co-accessibility showing with annotation of DCs (red), showing that *TNFAIP3* and *WAKMARK2* lie within a DC. (d) Gene expression of *TNFAIP3* TRG.



Supplementary Fig. 4. Comparison of co-accessibility analyses using ArchR, Cicero, and RWireX at the *TNFAIP3/IFNGR1/WAKMAR2* TRG cluster. (a) ArchR and Cicero co-accessibility at the *TNFAIP3/IFNGR1/WAKMAR2* TRG cluster. Top: pseudo-bulk chromatin accessibility. Middle: pseudo-bulk ATAC peaks extended to 1 kb (black), DCs from RWireX-meta (red), H3K27ac peaks at 30 minutes TNF (green), TRGs (blue), 1 kb regions surrounding their TSSs (light blue), and other genes (grey). Bottom: Co-accessibility links across all conditions from ArchR and per condition from Cicero. Co-accessibility links from ArchR revealed highly interconnected peaks within the RWireX-detected DC. Additionally, similar to RWireX-meta, several ArchR co-accessibility links connected the DCs with the upstream *IFNGR1* region. In contrast, Cicero co-accessibility links connected peaks throughout the genomic region without specific enrichment in the RWireX-detected DCs and the *IFNGR1* region. (b) Number of CCANs from Cicero and DCs from RWireX-meta, with colors reflecting the overlap between CCANs/DCs detected by Cicero and RWireX-meta. Cicero-identified cis-co-accessibility networks (CCANs) with a 60-67% overlap with DCs from RWireX-meta, although only half as many CCANs were detected genome-wide compared to DCs. (c) Genomic sizes of CCANs from Cicero, DCs from RWireX-meta, and TADs from HiC-seq data. The size distribution shows that CCANs are distinctly larger than DCs and more comparable to TADs detected from bulk HiC-seq data, indicating that RWireX-meta identifies chromatin compartments at higher resolution than existing methods.



Supplementary Fig. 5. Parameter optimization for RWireX-meta analysis. The evaluation of key parameters for domain detection is shown for the TRG cluster of *TNFAIP3*, *IFNGR1*, and *WAKMAR2* as an exemplary genomic region. The annotations include DCs (red), H3K27ac peaks at 30 min (green), TRGs (blue), 1 kb regions surrounding their TSSs (light blue), and other genes (grey). (a) Reference co-accessibility map (top), chromatin contacts from Hi-C-seq (bottom), and DC computed using optimized parameters (middle): RWireX-meta with 10 kb resolution and metacells aggregated from all three TNF treatment time points (0, 30, and 240 min). (b) Impact of reduced cellular variability on co-accessibility signal illustrated for the analysis of single time points for untreated cells (top) and 30 min TNF-treated cells (bottom). The lack of biological variation at the two individual time points led to more scattered co-accessibility correlations, and domains were not reliably detected. (c) Effect of high-resolution analysis using either 1 kb ATAC peaks (top) or 1 kb genomic tiles (bottom). The increased genomic resolution led to a low signal-to-noise ratio and a DC structure was only faintly visible. (d) Comparison of alternative tile sizes: 5 kb tiles (top) show reduced signal strength, and 20 kb tiles (bottom) showed loss of local features. The analysis demonstrates that 10 kb resolution (panel a) provided an optimal balance between signal quality and genomic resolution for detecting DCs.